

## Extended x-ray-absorption fine structure: Direct comparison of absorption and electron yield

Tie Guo and M. L. denBoer

*Department of Physics, Polytechnic Institute of New York, Brooklyn, New York 11201*

(Received 10 December 1984)

Using a simple ionization detector to monitor the total electron yield, we have measured extended x-ray-absorption fine structure above the Ni, Fe, and Cr *K* edges in the x-ray region. This technique is somewhat surface sensitive; we estimate a sampling depth of about 1000 Å. The fact that these materials do not differ from the bulk over this depth allows direct comparison with conventional absorption measurements. We find that interatomic spacings determined from the yield agree well with those measured by absorption. However, amplitudes differ significantly. These results have implications for the extraction of coordination numbers from the surface-sensitive variants of extended fine structure which monitor the electron yield. Finally, the electron-yield detector used here, employing conventional x-ray monochromators and not requiring elaborate precautions to prepare pristine surfaces, should prove useful in the study of, e.g., plated specimens or catalysts.

### I. INTRODUCTION

Extended x-ray-absorption fine structure (EXAFS) has become established as a useful ancillary tool in determining the physical structure of many materials.<sup>1,2</sup> The technique consists of analyzing the fine structure extending several hundred electron-volts above atomic absorption edges in the x-ray binding-energy range to extract interatomic spacings and coordination numbers. Two different methods are commonly employed to measure such extended fine structure for bulk samples. In concentrated samples which can be prepared as a suitably thin foil, the transmission method, in which the absorption of the sample is measured as a function of incident x-ray energy, is usually employed. For atoms present in the host in low concentrations the fluorescence technique, in which the fluorescent yield resulting from the recombination of the core holes created by the incident x rays is measured,<sup>3</sup> is often used. Surfaces can also be analyzed, by making use of the short mean free path of electrons in solids. The total or partial electron yield,<sup>4,5</sup> or the Auger yield,<sup>6</sup> due to the refilling of core holes created in the sample by the incident electron beam, or the photoyield,<sup>7</sup> may be measured as a function of incident photon energy. These electron-yield techniques rely on the expectation, first pointed out by Gudat and Kunz,<sup>8</sup> that the electron yield is proportional to the photon absorption cross section. Here we test this assumption in the x-ray region by comparing quantitatively total-electron-yield measurements of extended fine structure above the *K* edges of Ni, Fe, and Cr with conventional absorption.

### II. EXPERIMENT

The total-electron-yield technique we used, recently described by Kordesh and Hoffman,<sup>9</sup> is essentially an ionization detector with an internal sample, as also used in conversion electron Mössbauer spectroscopy.<sup>10</sup> This is somewhat surface sensitive, as we discuss below, but simple compared to surface EXAFS techniques. It relies on

the fact that the absorption length of electrons in a gas is much shorter than that of x rays of similar energy. Thus an amount of gas sufficient to completely absorb electrons will transmit x rays essentially entirely. This leads to the experimental geometry shown in the inset of Fig. 1. The sample forms the back of a He-filled chamber about 1 cm deep. The incident monochromatic x-ray beam enters through a Kapton window on the opposite side. As an ex-

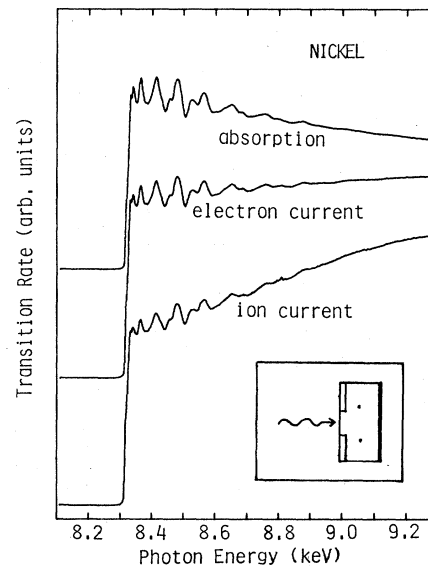


FIG. 1. Top curve is the absorption rate as measured in transmission of a Ni foil. This is compared to the total electron yield measured using the detector shown in the inset, which consists of a He-filled box with a Kapton window, through which photons strike the sample forming the opposite side. Two thin wires collect either the electron current, if positively biased, or the ion current, if negatively biased, with respect to the sample. A straight-line background fitted to the data below the Ni *K* edge has been removed from all three measurements and they have been normalized to unity jump at the edge to facilitate comparison. Note how the first few EXAFS oscillations are reduced in amplitude relative to the absorption.

ample, consider x rays with energy just above the iron  $K$  ( $1s$ ) core level incident on an iron sample. The iron  $K$  holes produced decay primarily by fluorescence, but a small fraction, typically 1% to 10% in this energy range,<sup>11</sup> decay by an Auger process, emitting electrons with a kinetic energy of several KeV. While both the incident and fluorescent x rays pass through the He, they are only weakly absorbed because of their long absorption length. However, the Auger and high-energy secondary electrons which leave the sample are completely absorbed, and essentially all their kinetic energy goes into the production of ion-electron pairs in the He. Two 0.1-mm wires placed so they are protected from the incident x-ray beam collect either the electrons or the ions produced, depending on their bias (25 to 100 V) with respect to the sample chamber. The current can be measured with the same electrometer technique used for gas-flow ionization detectors in conventional EXAFS. While secondary electrons produced in the sample by fluorescent x rays may also contribute to the signal, this term is expected to be small because such x rays are less energetic than the core level from which they are produced. Thus their absorption length in the same material is much longer, and most will leave the sample without exciting many secondary electrons.

The absorption data given here were taken on beam line II-3 at the Stanford Synchrotron Radiation Laboratory operating in dedicated mode, using a Si(111) channel-cut crystal monochromator. In Fig. 1 we compare a conventional transmission EXAFS measurement on a 10- $\mu$ m Ni foil to the corresponding electron- and ion-yield measurements. The transmission is, as customary, the log of  $I_0/I$ , where  $I_0$  is the incident x-ray flux measured by a separate ionization detector, and  $I$  is the transmitted flux. The Auger electron and ion-yield data are simply the ratio of the electron current to  $I_0$ . A typical electron current was  $10^{-10}$  A, and this increases by about a factor of 3 above the edge. The current increases with incident photon energy, as the total electron yield is an increasing function of energy. To facilitate comparison, we have therefore subtracted a linear fit to the pre-edge data in all cases, and normalized the data to unit jump at the edge. The ion-yield signal is considerably smaller, and hence noisier, than the electron-yield signal, as is also the case for ionization detectors. We therefore concentrate in the following on the electron yield.

### III. RESULTS

It is evident from Fig. 1 that the extended fine-structure oscillations are essentially the same, regardless of how they are measured. Both in position and in amplitude, the features of the transmission plot are reproduced in the electron and ion yield. This implies that interatomic spacings deduced from the oscillations will be the same. One significant difference is immediately apparent, however. The extended fine-structure oscillations have smaller amplitude in the electron case than in the transmission case; this reduction is even more marked for the ion yield. We quantify this difference below.

The oscillatory part of the transition rate  $\chi(k)$  is given for a  $K$ -absorption edge and a particular atomic shell by

$$\chi(k) = -k^{-1}A(k)\sin[2kr + \psi(k)] \quad (1)$$

with

$$A(k) = Nr^{-2}f(k, \pi)\exp(-2\sigma^2k^2 - 2r/\lambda). \quad (2)$$

Here  $f(k, \pi)$  is the backscattering amplitude and  $\psi(k)$  the total phase shift due to photoelectron scattering from a particular shell of  $N$  atoms located a distance  $r$  from the absorbing atom. The exponential terms in Eq. (2) are a Debye-Waller-like factor which accounts roughly for thermal vibrations, and a damping term to account for absorption. The wave vector of the ejected photoelectron  $k$  is defined as

$$k = \hbar^{-1}[2m(E - E_0)]^{1/2},$$

where  $E$  is the energy of the incident x ray and  $E_0$  essentially the binding energy of the core level. Customarily,  $\chi(k)$  is extracted from the experimental data by fitting and subtracting a smooth function from the absorption above the edge, and normalizing the remainder to the edge jump height.<sup>2</sup> Taking a Fourier transform isolates contributions from each atomic shell. In Fig. 2 we plot the conventional magnitude of the Fourier transform of  $k^3\chi(k)$  as a function of  $r$  as measured by absorption, electron yield, and ion yield. Peaks in the Fourier transform correspond to contributions from shells of Ni neighbors at various distances. In Fig. 2 the first three atomic shells are apparent. The peaks as obtained by the three techniques are evidently in very nearly the same locations. The reduction in amplitude in going from transmission through electron yield to ion yield is also evident.

We have performed similar measurements on Fe and Cr foils. In all cases, the transmission and electron-yield results were qualitatively similar. To quantify the differences observed, we use a modeling approach.<sup>2</sup> A particular peak in the Fourier transform is filtered out using a smooth window function and backtransformed into  $k$

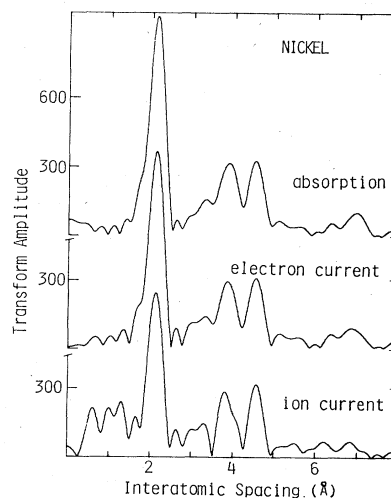


FIG. 2. Fourier transform of  $k^3\chi(k)$  obtained from the three measurements described in Fig. 1. All peaks are in essentially the same positions, indicating that interatomic spacings obtained from the three techniques will be the same. However, their relative amplitudes differ, making coordination-number comparisons difficult.

TABLE I. Results of fitting several peaks in the transforms plotted in Fig. 2, using Eqs. (1) and (2). Tabulated are the differences between the values obtained from the transmission measurement and the corresponding values for electron current (*e*) or ion current (*i*) in the detector, as described in the text.

| Material | Peak no. | Mode     | $r_a - r_e$<br>( $\text{\AA} \times 10^4$ ) | $(E_0)_a - (E_0)_e$<br>(eV) | $N_e/N_a$ | $\sigma_a^2 - \sigma_e^2$<br>( $\text{\AA}^2 \times 10^4$ ) |
|----------|----------|----------|---|-----------------------------|-----------|---|
| Ni       | 1        | <i>e</i> | 31  | 0.7                         | 0.78      | 9   |
|          |          | <i>i</i> | 31  | -1.0                        | 0.57      | 20  |
|          | 3        | <i>e</i> | 7   | -0.2                        | 0.76      | 12  |
|          |          | <i>i</i> | -9  | 1.0                         | 0.53      | 31  |
|          | 4        | <i>e</i> | -53   | -0.5                        | 0.79      | 11  |
|          |          | <i>i</i> | -18   | -1.6                        | 0.48      | 37  |
| Fe       | 1        | <i>e</i> | 6   | 0.2                         | 0.78      | 3   |
|          | 2        | <i>e</i> | 6   | 0.2                         | 0.78      | 3   |
|          | 4        | <i>e</i> | 22  | -0.1                        | 0.68      | 14  |
| Cr       | 1        | <i>e</i> | -55   | -0.5                        | 0.97      | -1  |
|          | 2        | <i>e</i> | -53   | -0.4                        | 0.97      | -1  |
|          | 4        | <i>e</i> | -30   | 0.0                         | 0.99      | -14   |

space, yielding oscillations due to one shell of atoms as given in Eq. (1). To compare the different measurements, we then extract the backscattering amplitude and phase shift from the transmission data and use them to fit the corresponding electron- and ion-yield data, neglecting mean-free-path differences and using as free parameters  $r$ ,  $E_0$ ,  $N$ , and  $\sigma^2$ .

The results are tabulated in Table I. The first column lists the difference between the value of  $r$  assumed in extracting phase shifts from the transmission data and that obtained in the fit to the yield. The second column lists the difference between corresponding values of  $E_0$ . As differences in  $r$  are consistently less than 0.005  $\text{\AA}$  and differences in  $E_0$  are small, it is evident that spacings obtained from the yield agree to well within usual EXAFS accuracy with those obtained from absorption. However, amplitude agreement, which determines the accuracy of coordination number measurements  $N$ , is less satisfactory. Column three is essentially the ratio of  $N$  obtained from

the transmission absorption measurement to that measured in the yield. Column four is the difference between  $\sigma^2$  measured from the yield and from the absorption. The differences seen here reflect the differences noted earlier in the amplitude of the extended fine-structure oscillations. Ni and Fe fine structure measured by electron yield is consistently about 20% smaller in amplitude than that obtained by absorption (indeed, even more for ion current on Ni), and it falls off more slowly with increasing  $k$ , as indicated by the  $\sigma^2$  differences. However, for Cr the amplitudes are very nearly the same.

The  $k$  dependence of the amplitude difference is indicated in Fig. 3, where we have compared the amplitude of the oscillations due to the nearest-neighbor peak in Ni as measured in absorption to that obtained from the electron current and the ion current. It is evident that the latter are below the absorption only for  $k < 10 \text{\AA}^{-1}$ ; beyond that, all three measurements are essentially the same.

#### IV. DISCUSSION

The agreement between the techniques on the interatomic spacings is excellent. However, the amplitude differences are disturbing, and it is worth speculating about possible causes. The well-known thickness effect<sup>12</sup> causes a decrease in measured EXAFS amplitude for thick samples measured in absorption. Our samples are less than 10  $\mu\text{m}$  thick, and in any case this effect reduces amplitude in absorption. In yield measurements we are always in the thin limit, as the absorption length of the incident x rays is much longer than the sampling depth. The good agreement in atomic spacings indicates that there are no significant differences between the bulk and the surface region sampled by the electron-yield measurements. Furthermore, we compared different sides of the Ni and Fe foils, which showed different amounts of oxidation, but gave identical results.

Amplitude differences between electron yield and ab-

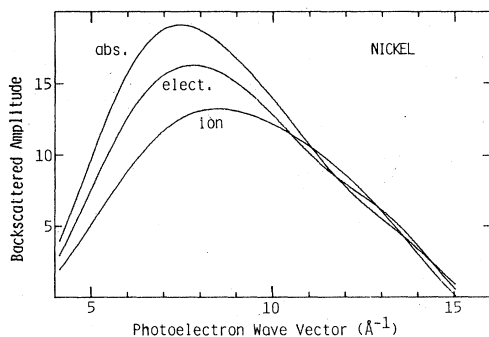


FIG. 3. Amplitude of the first-neighbor peak in each of the three cases of Fig. 1. These were obtained by filtering the first peak and backtransforming into  $k$  space. The amplitude is considerably smaller in the electron- and ion-current  $k$  data for  $k < 10 \text{\AA}^{-1}$ .

sorption have been previously observed for the Cu *K* edge by Martens *et al.*<sup>13</sup> Stohr *et al.*<sup>14</sup> observed a reduction of the EXAFS amplitude above the Al *K* edge (1540 eV) in total electron yield as compared to Auger electron yield, and suggested this reduction was due to a contribution to the signal in the total-yield case from inelastically scattered photoelectrons which did not carry EXAFS information, which contribution increases with energy above the edge. However, we believe for several reasons that this is not a satisfactory explanation at 1500 eV, and certainly not at 7000 eV.<sup>15</sup> First of all, this model predicts greater amplitude differences high in energy above the edge; in contrast, we see the greatest differences near the edge. Secondly, it is not clear why inelastic photoelectrons should not also carry EXAFS information. Finally, at the high-binding-energy levels measured here the differences in secondary electron yield between photoelectrons and Auger electrons (which in this model are responsible for the EXAFS amplitude differences between transmission and electron-yield techniques) should be negligibly small. We do not have an explanation for this phenomenon, but are inclined to suspect something related more directly to the measurement, noting that a greater amplitude difference is observed in the ion-current measurement and that the Cr measurements are in good internal agreement.

The electron-yield measurement is a surface-sensitive probe, because of the short mean free path and hence escape depth of electrons in solids. The actual sampling depth in these high-energy total-yield measurements is difficult to estimate with any degree of precision. In surface-analysis techniques such as photoemission and Auger electron spectroscopy, the sampling depth is simply related to the escape depth of the low-energy (ordinarily under 1 keV) electrons used, because electrons which have suffered an inelastic loss during their exit from the sample are not included in the measured signal. Experiments suggest the escape depth  $l$  has the form

$$l \propto E_{\text{kin}}^{\alpha},$$

where  $E_{\text{kin}}$  is the electron kinetic energy and values of  $\alpha$  between 0.5 and 0.66 have been proposed.<sup>16-18</sup> Using  $\alpha=0.5$  and the value at the Mg *K* $\alpha$  photon energy from Ref. 17,  $l$  is about 50 Å at 7 keV, a typical energy for 3d transition metal *KLL* Auger electrons. This is, of course, an extrapolation from measurements at energies primarily below 1.5 keV.

The actual sampling depth here is much deeper than this, however, because electrons can contribute to the measured signal even after having suffered an inelastic collision. Furthermore, the initial Auger electron causes a cascade of low-energy electrons. Essentially, the sample is used as an electron multiplier. All electrons which emerge from the sample with sufficient kinetic energy to ionize a He atom will be measured. Given the shape of the He ionization cross section, this means largely electrons above 50 eV. Jones and Woodruff<sup>19</sup> estimated the sampling depth in total yield for the Al *K* edge at 390 Å, by observing the effects of oxidation. Martens *et al.*<sup>13</sup> estimated several hundred Å for the Cu *K* edge by measur-

ing the signal as a function of incident angle. A possibly significant difference is that those experiments involved counting discrete pulses from each individual photoabsorption event, so that in principle an absorption event which results in only one secondary electron contributes equally with one which produces a hundred secondaries, while here we measure a current which is proportional to the number of secondary electrons produced by each photoabsorption event. This suggests our surface sensitivity may be somewhat greater. An upper limit to the sampling depth may be obtained by considering the case of a 7-keV electron traveling directly toward the surface which loses 50 eV per mean free path. This is not so farfetched, as the creation of low-energy excitations is the primary energy-loss mechanism of electrons in solids. After 100 loss events, this electron would be left with 2 keV of energy and have traveled some 4000 Å. Allowing for angular dispersion and the fact that most of the secondary electrons thus produced would not reach the surface, this suggests a sampling depth of somewhat less than 1000 Å.

## V. CONCLUSIONS

The most encouraging result of these measurements is that total-electron-yield techniques give excellent agreement with absorption on interatomic spacings. Thus, in experiments using variants of surface EXAFS, phase information obtained from total-yield measurements, which are often the technique of choice because of the generally higher signal, may be reliably applied to unknown systems. However, as amplitude differences are apparently present, coordination numbers should be treated with even more caution than is normally required.

The simple electron-yield detector used here should have other uses. Evidently, it is useful in studying systems which have surfaces that are interesting over a depth of 1000 Å or so. Examples include working catalysts, plated specimens, and small particles. It is also suitable for systems which cannot be made into the thin foils required for absorption; one is always in the thin limit. The signal is reduced from absorption, firstly by the ratio of the sampling depth ( $10^{-7}$  m) to the sample thickness in absorption ( $10^{-6}$  m) or 10%, and secondly by the Auger decay fraction, about 10% to 1% in the energy range studied here. As this fraction decreases with increasing energy, high-binding-energy levels should be more difficult. We had no difficulty, however, measuring EXAFS associated with the Zr *K* edge at 18 keV. As with absorption, the signal is proportional to the area of the incident beam, all else being equal. In some cases, this detector may be a good alternative to fluorescence detection,<sup>3</sup> commonly employed to measure elements at low concentrations. Offsetting the signal-reducing factors mentioned above is the effectively  $2\pi$  solid angle for collection, much larger than anything achievable in fluorescence, and the unlimited counting rate, unless one uses an ionization chamber and gives up energy resolution. There are also no absorption effects to worry about. However, no energy analysis of the signal is possible to increase the signal-to-background ratio.

## ACKNOWLEDGMENTS

This work was supported by the National Science Foundation (Solid State Chemistry Program), under Grant No. DMR-83-06426. Stanford Synchrotron Radiation Laboratory (SSRL) is supported by the Office of

Basic Energy Sciences of the U. S. Department of Energy and the Division of Materials Research of the National Science Foundation. We appreciate sample loans and illuminating discussions with Mathew Marcus, and assistance from Brian Kincaid.

- 
- <sup>1</sup>D. E. Sayers, E. A. Stern, and F. W. Lytle, *Phys. Rev. Lett.* **27**, 584 (1971).
- <sup>2</sup>P. A. Lee, P. H. Citrin, P. Eisenberger, and B. M. Kincaid, *Rev. Mod. Phys.* **53**, 769 (1981).
- <sup>3</sup>J. B. Hastings, *J. Appl. Phys.* **48**, 1576 (1977).
- <sup>4</sup>J. Stöhr, D. Denley, and P. Perfetti, *Phys. Rev. B* **18**, 4132 (1978).
- <sup>5</sup>J. Stöhr, R. S. Bauer, J. C. McMenamin, L. I. Johansson, and S. Brennan, *J. Vac. Sci. Technol.* **16**, 1195 (1981).
- <sup>6</sup>P. H. Citrin, P. Eisenberger, and R. C. Hewitt, *Phys. Rev. Lett.* **41**, 309 (1978).
- <sup>7</sup>G. M. Rothberg, K. M. Choudhary, M. L. denBoer, G. P. Williams, M. H. Hecht, and I. Lindau, *Phys. Rev. Lett.* **53**, 1183 (1984).
- <sup>8</sup>W. Gudat and C. Kunz, *Phys. Rev. Lett.* **29**, 169 (1972).
- <sup>9</sup>M. E. Kordesh and R. W. Hoffman, *Phys. Rev. B* **29**, 491 (1984).
- <sup>10</sup>See, for example, W. Jones, J. M. Thomas, R. K. Thorpe, and M. J. Tricker, *Appl. Surf. Sci.* **1**, 388 (1978).
- <sup>11</sup>Uzi Landman and David L. Adams, *Proc. Nat. Acad. Sci. U.S.A.* **75**, 2550 (1976); E. J. McGuire, *Phys. Rev. A* **2**, 273 (1970).
- <sup>12</sup>E. A. Stern and K. Kim, *Phys. Rev. B* **23**, 3781 (1981).
- <sup>13</sup>G. Martens, P. Rabe, N. Schwenter, and A. Werner, *J. Phys. C* **11**, 3125 (1978).
- <sup>14</sup>J. Stöhr, C. Noguera, and T. Kendelewicz, *Phys. Rev. B* **30**, 5571 (1984).
- <sup>15</sup>M. L. denBoer (unpublished).
- <sup>16</sup>M. P. Seah and W. A. Dench, *Surf. Interface Anal.* **1**, 2 (1979).
- <sup>17</sup>C. D. Wagner, L. E. Davis, and M. Riggs, *Surf. Interface Anal.* **2**, 53 (1980).
- <sup>18</sup>S. -J. Oh, J. W. Allen, and I. Lindau, *Phys. Rev. B* **30**, 1937 (1984).
- <sup>19</sup>R. G. Jones and D. P. Woodruff, *Surf. Sci.* **114**, 38 (1982).